PHILOSOPHICAL TRANSACTIONS OF THE ROYAL SOCIETY A MATHEMATICAL, PHYSICAL & ENGINEERING SCIENCES

Ionization Fronts in Interstellar Gas: The Structure of Ionization Fronts

W. I. Axford

Phil. Trans. R. Soc. Lond. A 1961 **253**, 301-333
doi: 10.1098/rsta.1961.0002

IONIZATION FRONTS IN INTERSTELLAR GAS: THE STRUCTURE OF IONIZATION FRONTS

By W. I. AXFORD†

Department of Mathematics, Manchester University

(*Communicated by M. J. Lighthill, F.R.S.—Received 29 March 1960*)

CONTENTS

A complete analysis of the structures of all types of ionization front is given, together with computed examples. It is shown that the solutions given by Goldsworthy for the propagation of ionization fronts, considered as discontinuities, can be made unique, and the unique solutions are given for the case of cylindrical symmetry. Ionization fronts of all types are shown to be possible, depending on the density of the ionized gas and the spectral type of the radiation. In particular strong *D*-type and weak *R*-type ionization fronts (corresponding to strong deflagrations and weak detonations, respectively, in combustion theory) prove to be of importance. The existence of these discontinuities conflicts with the Chapman–Jouguet hypothesis and the reasons for this behaviour are examined in detail. It is concluded that the most important condition for waves of this type to occur is that strong cooling effects should be present, which allow the stagnation enthalpy of the flow to have a maximum before decreasing to an equilibrium value at the rear of the wave. It is suggested that this may be of significance in the theory of other gas-dynamic discontinuities, and in determining the validity of the Chapman–Jouguet hypothesis in general.

NOTATION

a adiabatic sound speed, (2·5)
A a constant, (3·4)
B a constant, (3·4)
c the (isothermal) sound speed in the H II region, (1·9) and (2·6)

† Present address: Defense Research Board Telecommunication Establishment, Shirley Bay, Ottawa.

d	equals ± 1, (3·9b)
D	a constant, (3·7)
e	equals ± 1, (3·5)
E	a constant, (3·14), and also stagnation enthalpy per unit mass, (5·3)
G	(non-dimensional) stagnation enthalpy, (3·8)
H	function of temperature, (3·15)
j	(non-dimensional) flux of ionizing photons, (3·10)
J	flux of ionizing photons
J_*	flux of ionizing photons at the stellar surface
k	Boltzmann's constant
m	the mass flow across a gas-dynamic discontinuity
M	mass of a hydrogen atom
M_1, M_2	Mach numbers, (3·18a, b)
N	number density of neutral hydrogen atoms
p	pressure
P	the momentum flux across a gas-dynamic discontinuity
r	distance from the stellar surface
r_i	radius of H II region
R_*	radius of star
S	entropy per unit mass
S, S', S''	limiting values of U_i/c for various types of ionization front, §§ 4·1, 4·2
t	time
T	temperature in degrees Kelvin
T_c	temperature of the H II region, (1·8)
T_*	colour temperature of star
u	gas velocity in r-direction
U_i	speed of ionization front
v	gas velocity relative to the ionization front
$\overline{w}$	non-dimensional variable, proportional to $\overline{v}$, (3·5b)
x	fraction of ionized atoms
Y	non-dimensional variable, (3·7)
z	density ratio, (2·7)
α	approximate absorption coefficient
$\beta_0/T^{\frac{3}{4}}$	approximate recombination coefficient
γ	ratio of specific heats (equals 5/3)
Δ	thickness of ionization front
ϵ	fraction of 'burnt' gas, (5·3)
θ	(non-dimensional) temperature, (3·4)
ρ	density
σ	Bohr diameter of the hydrogen atom
τ	specific volume
ϕ	(non-dimensional) length scale, (3·17)
ω_0	density parameter in Goldsworthy's solutions, § 1·1

PHILOSOPHICAL TRANSACTIONS OF THE ROYAL SOCIETY A MATHEMATICAL, PHYSICAL & ENGINEERING SCIENCES

The equations defining the symbol, or the sections where it is of most importance, are given above where necessary. The inclusion of a bar (e.g. $\bar{\rho}$) denotes a quantity which has been made non-dimensional (see § 3). The following subscripts are also used:

0 referring to values in the undisturbed H I region,
1 referring to values ahead of the ionization front,
2 referring to values behind the ionization front,
i referring to values at the ionization front.

The index n has the values 0, 1, 2 for the cases of plane, cylindrical, and spherical symmetry, respectively.

1. Introduction

Following the discovery by Struve & Elvey (1938) of large regions of ionized hydrogen in the Milky Way, Strömgren (1939) examined the effects of ionizing radiation emitted by a young hot star on the surrounding interstellar gas. Dynamical effects were completely neglected in this investigation, but the results are important because they show that the gas is divided into a spherical fully ionized (H II) region surrounding the star, and an unionized (H I) region. These regions are separated by an 'ionization front' which is thin compared with the dimensions of the H II region. The structure of the ionization front can be found quite easily in this case but, as there is no mass motion, the results are not of great interest.

Several attempts were made to allow for dynamical effects in the development of H II regions, but until Kahn (1954) made his investigation of Oort & Spitzer's (1955) 'rocket effect', there was no satisfactory account of the motion of material across the ionization front. Kahn gave equations representing the conservation of mass, momentum and energy across the ionization front, and showed that there is a close analogy between combustion waves and ionization fronts. The terms '*R*-type' and '*D*-type' were first used in this work to distinguish between ionization fronts corresponding to detonations and deflagrations, respectively.

Goldsworthy (1958, 1961) has used Kahn's equations to examine the development of H II regions around line and point sources of radiation. A certain density distribution in the undisturbed H I region is required in order to make a similarity solution possible, but despite this drawback, the solution represents a considerable improvement on earlier attempts by other writers. Flows containing weak and strong *R*-type and *D*-type† ionization fronts are found to occur, depending on the spectral type of the source of radiation, and the density of the unionized gas. The flow pattern in any case is not unique, however, as an infinity of patterns with a strong *D*-type ionization front can occur, together with a single pattern containing one of the other three types, for any given density in the H I region and spectral type of star. Goldsworthy has made further improvements on this work, by allowing for recombination of electrons and protons and also for cooling due to the excitation of O^+ ions, these effects being neglected by Kahn. The cooling mechanism is that suggested by Spitzer (1954), and together with recombination, it keeps the temperature of the H II region practically uniform at a value in the range 7000 to 10 000 °K,

† The reader who is unfamiliar with this classification of the types of ionization front should refer to § 2 of this paper.

PHILOSOPHICAL TRANSACTIONS OF THE ROYAL SOCIETY A MATHEMATICAL, PHYSICAL & ENGINEERING SCIENCES

depending on the spectral type of the exciting star. Shocks occurring in the H II region are so strongly affected by this cooling that they can be regarded as being isothermal. The gas velocities obtained in this case are found to be of the order of the thermal velocity in the H II region, rather than the thermal velocity corresponding to the colour temperature of the star, as found in the case with recombination and cooling neglected. The flow patterns are the same however, and there is still a lack of uniqueness in the solution.

One of the aims of this paper to to remove the lack of uniqueness in Goldsworthy's solutions. The analysis of ionization front structures shows that there is only one possible flow pattern for each combination of the density in the H I region and spectral type of radiation. The most interesting result of this work is that ionization fronts occur which would be forbidden in combustion theory by the Chapman–Jouguet hypothesis. This point is dealt with at length in § 5, where it is shown that for strong deflagrations and the associated weak detonations (containing a shock) to be possible, there must be an endothermic section in the structure of the wave, as well as a suitable external flow. The author believes that, in certain circumstances, a combustion process with strong cooling effects associated with it could produce a non-Chapman–Jouguet wave. Unfortunately, apart from some work by Taylor (1950) on spherical detonation, little work appears to have been done on anything but one-dimensional propagation of gas-dynamic discontinuities, and also, as diffusive effects such as viscosity and heat conduction are so important in many cases, a complete analysis of the structure of these waves would be very difficult to carry out. The work of Goldsworthy, together with results of this paper, should therefore prove of considerable interest, as it is the only case in which a full examination has been made of both the propagation and the structure of any sort of gas-dynamic discontinuity.

1·1 Goldsworthy's solution for the flow in the large

The partial differential equations which describe the development of an ionized region around a star have been given by Goldsworthy (1960). They are:

absorption of ionizing photons
$$\frac{1}{r^n}\frac{\partial}{\partial r}(Jr^n) = -\frac{\alpha}{M}J\rho(1-x), \tag{1·1}$$

ionization balance
$$\frac{\mathrm{D}x}{\mathrm{D}t} = \alpha J(1-x) - \frac{\beta_0}{M}\frac{\rho x^2}{T^{\frac{3}{4}}}, \tag{1·2}$$

equation of state
$$p = \frac{k}{M}(1+x)\rho T, \tag{1·3}$$

conservation of momentum
$$\frac{\mathrm{D}u}{\mathrm{D}t} = -\frac{1}{\rho}\frac{\partial p}{\partial r}, \tag{1·4}$$

continuity
$$\frac{\partial \rho}{\partial t} + \frac{1}{r^n}\frac{\partial}{\partial r}(r^n\rho u) = 0, \tag{1·5}$$

conservation of energy
$$\frac{\mathrm{D}}{\mathrm{D}t}\left(\frac{3p}{2\rho}\right) - \frac{p}{\rho^2}\frac{\mathrm{D}\rho}{\mathrm{D}t} = \frac{\alpha k T_*}{M}J(1-x) - \tfrac{3}{2}k\beta_0 T^{\frac{1}{4}}\frac{\rho x^2}{M^2} - \frac{\rho x^2}{M^2}L_{ci}, \tag{1·6}$$

where
$$L_{ei} = 0{\cdot}97\times 10^{-31}(T-4000)^2 \quad \text{for} \quad T \geqslant 4000\,^\circ\mathrm{K}$$
$$= 0 \quad \text{for} \quad T < 4000\,^\circ\mathrm{K}, \tag{1·7}$$

and the operator $\mathrm{D}/\mathrm{D}t$ is a contraction of $\{\partial/\partial t+u(\partial/\partial r)\}$. The index n has the value 0, 1, 2 according as the problem is assumed to have plane, cylindrical, or spherical symmetry. It is convenient to define a typical temperature T_c, as the value of T which makes the following expression zero,

$$\left\{T_* - 1{\cdot}5T - \frac{T^{\frac{3}{4}}}{\beta_0 k} L_{ei}\right\}. \tag{1·8}$$

Values of T_c have been given in Goldsworthy's paper, and they are found to lie in the range 7000 to 10 000 °K for different values of T_*.

The boundary conditions in a typical problem are

$$u = x = J = 0,$$

$$T = T_0(r), \quad \rho = \rho_0(r),$$

before the star begins to radiate at time $t = 0$. At subsequent times, the rate of output of ionizing photons from unit area of the star's surface is assumed to be given and is denoted by J_*.

Goldsworthy has considered problems with cylindrical and spherical symmetry in which $T_0(r) \ll T_c$, $u = 0$ at the star for all t, and $\rho_0(r)$ is chosen in such a way that a similarity solution is possible. Since the typical velocity c, in the problem, given by

$$c^2 = 2kT_c/M, \tag{1·9}$$

is constant, the similarity variable is $\eta = ct/r$, (1·10)

and hence the flow pattern moves out uniformly in time. The ordinary differential equations which result from equations (1·1) to (1·6) are extremely difficult to integrate, even with the aid of an electronic computer, and it was found necessary to adopt an approximate method. The assumptions involved in the method were discussed by Goldsworthy, and are as follows:

(i) Ionization is confined to an H II region surrounding the star, which is separated from the unionized gas by an ionization front of negligible thickness. Ahead of the front, ionization due to absorption of radiation, with consequent preheating of the gas, is neglected.

(ii) The gas in the H II region is almost fully ionized so that x can be put equal to unity, except in the factor $(1-x)$ which can be eliminated. The derivative $\mathrm{D}x/\mathrm{D}t$ is negligible.

(iii) The gas in the H II region is practically isothermal with temperature T_c, and this condition replaces the energy equation (1·6). Shocks in the H II region are isothermal, and the velocity of sound is c.

(iv) The ratio $J_i r_i^n / J_* R_*^n$ is assumed to be very small, where r_i is the radius of the H II region and J_i is the flux of ionizing photons at the ionization front.

(v) The absorption of photons in isothermal shocks is neglected so that J and x are continuous across flow discontinuities of this type.

(vi) Shocks in the H I region are assumed to be strong.

The application of these assumptions to equations (1·1) to (1·6) results in a great simplification, and the investigation of both cylindrical and spherical problems is made quite easy if the flow is assumed to be similar. The undisturbed density distributions required for

this are ω_0/r and $\omega_0/r^{\frac{3}{2}}$ for the cylindrical and spherical cases, respectively. The technique of solving these problems consists of assuming a flow pattern, and then finding the value of ω_0 which gives this flow pattern for given values of T_*. It is shown in Goldsworthy's paper that the relationship between flow pattern, ω_0 and T_*, is not unique and in fact, for each combination of ω_0 and T_*, there is a single infinity of possible flow patterns with two shocks and a strong D-type ionization front, and one other flow pattern with in general one shock and a weak R-type, weak D-type or strong R-type ionization front. An analysis of the structure of the ionization fronts is necessary to resolve this lack of uniqueness, and also to justify some of the assumptions made. The unique solution for the case of cylindrical

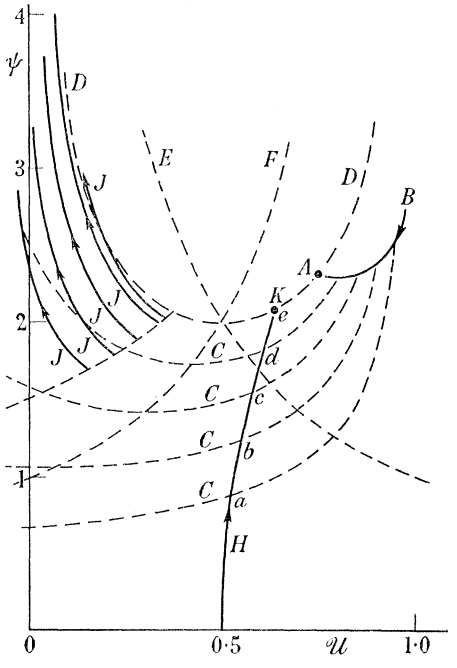

FIGURE 1. The solution for the external flow in the cylindrical problem, expressed diagrammatically in terms of integral curves in the $(\mathscr{U}, \psi)$ plane.

symmetry with $\rho_0(r) = \omega_0/r$ will be given in this paper. Similar calculations would give the unique solution in the spherical case. For a description of the flow 'in the large', the reader is referred to Goldsworthy's paper where the solutions are discussed in terms of a gas velocity–sound speed diagram (i.e. $\mathscr{U}/\mathscr{A}$ diagram). For the cylindrical case, this diagram is repeated in figure 1, where the ordinate is changed to

$$\psi = \left\{\frac{2T_c}{\eta^2(1+x)\,T}\right\}^{\frac{1}{2}} = \frac{1}{\mathscr{A}}. \tag{1·11}$$

There is a slight advantage in using this variable in that it is directly proportional to r in the ionized region.

The curves appearing in figure (1) may be described as follows. AB is the integral curve representing motion in the H I region behind a strong shock, A being the 'strong shock' point. The dashed lines, C, are the loci of possible transitions, via an ionization front, from various points on the strong shock curve. The single dashed curve, D, is the locus of points which can be reached by an ionization front transition from conditions in the undisturbed

H I region. The curves E and F are given by $\mathscr{U}\psi = 1$ and $(1-\mathscr{U})\psi = 1$, respectively. H is the integral curve representing shockless flow in the H II region, its intersection with D giving the only possible strong R-type ionization front (i.e. point K). The intersections of H with the transition lines C give a series of possible weak D-type ionization fronts (for example, a, b, c and d). Flows for which shocks occur in the H II region are represented by breaking off from the integral curve H, and moving to the curve G by means of an isothermal shock (ψ being constant in this transition); the remainder of the motion in the H II region is then represented by an integral curve starting at the appropriate point of G, some typical example of such curves being labelled J in the diagram. Some integral curves of the set J intersect D, giving a series of possible weak R-type ionization fronts, and the intersections of the set J with the transition curves C give possible strong D-type ionization fronts. Clearly, there are in all ∞^2 strong D-type, ∞ weak D-type and weak R-type, and only one strong R-type, patterns of flow. In the diagram, the star is situated on the abscissa, and the arrowheads on the integral curves indicate the radial direction.

2. Features of the ionization front transition

If the ionization front is treated as a mathematical discontinuity, the equations expressing continuity of mass and linear momentum are

$$\rho_1 v_1 = \rho_2 v_2 = m, \tag{2·1}$$

$$p_1 + \rho_1 v_1^2 = p_2 + \rho_2 v_2^2, \tag{2·2}$$

where suffixes 1, 2 refer to conditions upstream and downstream of the transition, respectively. These are exactly as for a shock wave, and can be combined to give

$$(p_2 - p_1) = -m^2(\tau_2 - \tau_1). \tag{2·3}$$

Usually a third equation representing conservation of energy across the transition can be written. However, Goldsworthy (1960) has shown that for an ionization front this must be replaced by the statement that the H II region is isothermal. That is,

$$T_2 = T_c, \tag{2·4}$$

where T_c is the equilibrium temperature calculated from the expression (1·8). It is convenient to define velocities c and c_1 which are representative of the flows in the H II and H I regions, respectively, as follows,

$$c_1^2 = p_1\tau_1 = kT_1/M = 3a_1^2/5, \tag{2·5}$$

$$c^2 = p_2\tau_2 = 2kT_c/M, \tag{2·6}$$

where a_1 is the velocity of sound in the H I region, and c may be regarded as the 'isothermal' velocity of sound for the H II region.

The transition will be considered in terms of a variable z, such that

$$\rho_2 = z\rho_1, \quad \tau_2 = \tau_1/z, \quad v_1 = zv_2. \tag{2·7}$$

The transition is called R-type if the density increases ($z > 1$), and D-type if the density decreases ($z < 1$). Equations (2·1), (2·2) and (2·3) reduce to

$$c^2z^2 - (c_1^2 + v_1^2)\, z + v_1^2 = 0. \tag{2·8}$$

This quadratic in z has real roots if

$$(c_1^2+v_1^2)^2 \geqslant 4c^2v_1^2. \tag{2·9}$$

The expression in (2·9) is a quadratic in v_1^2, which satisfies the inequality if v_1^2 lies outside

$$\{2c^2-c_1^2+2c(c^2-c_1^2)^{\frac{1}{2}},\ 2c^2-c_1^2-2c(c^2-c_1^2)^{\frac{1}{2}}\}.$$

There are three cases which will be treated separately.

(*a*) If $c^2 > c_1^2$, there is a range of v_1^2 which is forbidden by (2·9).

(*b*) If $c^2 = c_1^2$, (2·9) is always satisfied, and there is equality if $v_1^2 = c_1^2$.

(*c*) If $c^2 < c_1^2$, (2·9) is always satisfied and the equality does not occur.

In order to discuss these various cases, it is useful to consider the formula

$$z_1 \geqslant \frac{2z_1z_2}{z_1+z_2} \geqslant z_2, \tag{2·10}$$

where z_1 and z_2 are the roots of equation (2·8) and $z_1 \geqslant z_2$. Substituting from (2·8), this becomes

$$z_1 \geqslant \frac{2v_1^2}{c_1^2+v_1^2} \geqslant z_2. \tag{2·11}$$

Also, from (2·7) and (2·8) it is readily seen that

$$\frac{c^2}{v_2^2}-1 = \left(\frac{cz}{v_1}\right)^2-1 = \frac{c_1^2+v_1^2}{v_1^2}z-2. \tag{2·12}$$

Hence, for transitions corresponding to z_1, $v_2^2 < c^2$ and the ionization front moves subsonically relative to the fluid downstream. On the other hand, for the transition corresponding to z_2, $v_2^2 > c^2$ and the ionization front moves supersonically relative to the fluid downstream. In the special circumstances in which $z_1 = z_2$, the ionization front moves at sonic speed relative to the fluid downstream and the transition is called 'critical'.

The various possible transitions are discussed using the Hugoniot diagram,† which is simply a representation of equations (2·1), (2·2) and (2·4) in the (p, τ) plane. The 'Hugoniot curve', which is the locus of all possible combinations of p and τ which can occur behind an ionization front, is given by the hyperbola (2·6). The conditions ahead are represented by the point (p_1, τ_1) which is below, on, or above the Hugoniot curve, according as case (*a*), (*b*) or (*c*) is being considered. The straight line (2·3) represents transitions from the state (p_1, τ_1) to the state (p_2, τ_2), and it cuts the Hugoniot curve in points given by the roots of equation (2·8). Straight lines drawn from (p_1, τ_1) with positive slope do not represent transitions as they correspond to imaginary values of m, while lines of negative slope which do not cut the Hugoniot curve represent the transitions forbidden by (2·9) (these are called M-type transitions by Kahn (1954)).

Case (a)

The Hugoniot diagram for this case is shown in figure 2 where it can be seen that the Hugoniot curve has two branches, the upper branch representing R-type transitions, and the lower branch representing D-type transitions. Each branch is divided into weak and strong parts separated by a critical point. Strong R-type and weak D-type ionization fronts have $z = z_1$ and therefore move subsonically relative to the fluid behind. Weak R-type

† See Courant & Friedrichs (1948).

and strong D-type ionization fronts have $z = z_2$ and so move supersonically relative to the fluid behind. Both R- and D-critical ionization fronts move with sonic speed relative to the fluid behind.

Since $z < 1$ for all D-types, equation (2·11) shows that $v_1 < c_1 < a_1$ so that all D-type ionization fronts move subsonically relative to the fluid ahead. For R-type ionization fronts $z \geqslant 1$ and equation (2·11) shows that $v_1 \geqslant c_1$. Thus an R-type ionization front does not always move supersonically relative to the fluid ahead. The minimum velocity v_1 occurs when m is a minimum, that is, when the transition is critical. In this case

$$v_1^2 = 2c^2 - c_1^2 + 2c(c^2 - c_1^2)^{\frac{1}{2}}. \tag{2·13}$$

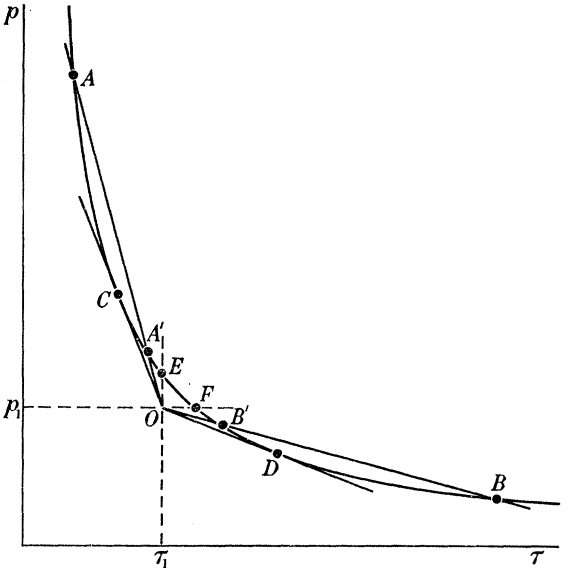

FIGURE 2. The Hugoniot diagram for case (*a*). Transition lines like $OA'A$ give weak R-type (OA') and strong R-type (OA) transitions, and those like $OB'B$ give weak D-type (OB') and strong D-type (OB) transitions. The two transition lines tangential to the Hugoniot curve give R-critical (OC) and D-critical (OD) transitions. Limiting cases are the constant-volume R-type (OE) and the constant-pressure D-type (OF).

Therefore, the motion is always supersonic relative to the fluid ahead if

$$4\gamma c^2 > (\gamma + 1)^2 c_1^2. \tag{2·14}$$

The constant-volume R-type with $m = \infty$, and the constant-pressure D-type with $m = 0$, can be regarded as being special cases of the weak D-type and weak R-type, respectively. For the constant pressure D-type, $v_1 = v_2 = 0$ and the H II region is static, while for the constant-volume R-type $v_1 = v_2 = \infty$ and ionization can be thought of as taking place instantaneously with no mechanical effects.

Case (b)

In this rather special case, the weak R- and D-types and the critical R- and D-types of case (*a*) have collapsed into a single transition in which the values of p, ρ and v do not change, but for which the temperature is halved. The roots of equation (2·8) are v_1^2/c_1^2 and 1. Hence if the transition is critical (that is, the transition line (2·3) is a tangent at (p_1, τ_1)), the

ionization front moves subsonically relative to the fluid ahead ($v_1 = c_1$) and with sonic speed relative to the fluid behind.

For the strong R- and D-types, the speed of the ionization front relative to the fluid ahead is given by

$$v_1^2 = zc_1^2. \tag{2·15}$$

Hence strong R-type ionization fronts for which $z > \gamma$ move supersonically relative to the fluid ahead, and the remaining strong R-types and all strong D-types move subsonically relative to the fluid ahead.

The motion relative to the fluid behind the ionization front is the same as for case (a).

The Hugoniot diagram for case (b) is shown in figure 3. Since all non-negative values of m are possible, Kahn's M-type conditions do not occur in this case.

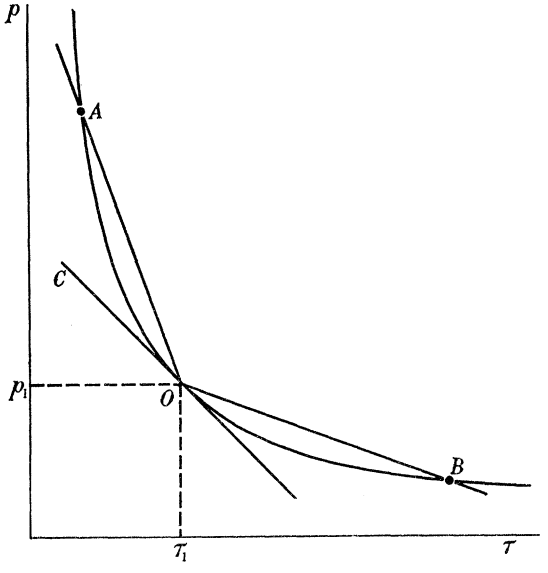

FIGURE 3. The Hugoniot diagram for case (b). Transition lines like OA and OB give strong R-type and strong D-type transitions, respectively. Transitions along OC form a degenerate set; they are critical R-type ($v_1 = c_1$, $v_2 = c$), weak R-type ($v_1 > c_1$, $v_2 > c$), weak D-type ($v_1 < c_1$, $v_2 < c$) and critical D-type ($v_1 = c_1$, $v_2 = c$).

Case (c)

In this case, the point (p_1, τ_1) lies above the Hugoniot curve, as shown in figure 4, and equation (2·8) has roots which lie on either side of unity. That is

$$z_1 > 1 \geqslant z_2.$$

The minimum value of z_1 is c^2/c_1^2, when the transition is a constant-pressure R-type. The maximum value of z_2 is unity, when the transition is a constant-volume D-type. The root z_1 always corresponds to a strong R-type ionization front, and the root z_2 always corresponds to a strong D-type ionization front. The weak and critical types of case (a) do not occur, and as in case (a) the R- and D-branches of the Hugoniot curve are separated by a short length which corresponds to imaginary values of m.

Since corresponding R- and D-types move with the same speed relative to the fluid ahead, both types can move subsonically or supersonically, but in all cases the strong R-types move

with subsonic speed relative to the fluid behind, and the strong D-types move with supersonic speed. Transitions can occur with all positive values of m, so that for a given value of τ_1 there is a value of m for which the ionization front moves into the fluid upstream with sonic speed. This is shown in figure (4) as the 'sonic' transition line. Transitions corresponding to lines of more negative slope will move supersonically, and those corresponding to lines of less negative slope will move subsonically, into the fluid ahead.

This description of the various possible types of ionization front is similar to that usually given for combustion waves, except that conservation of energy is not assumed. Cases (b) and (c) are considered not to occur for combustion waves, but for H II regions it must be recognized that the gas will be subject to strong cooling if it is above the equilibrium temperature. Indeed, this cooling may be so strong that the overall effect of the ionization

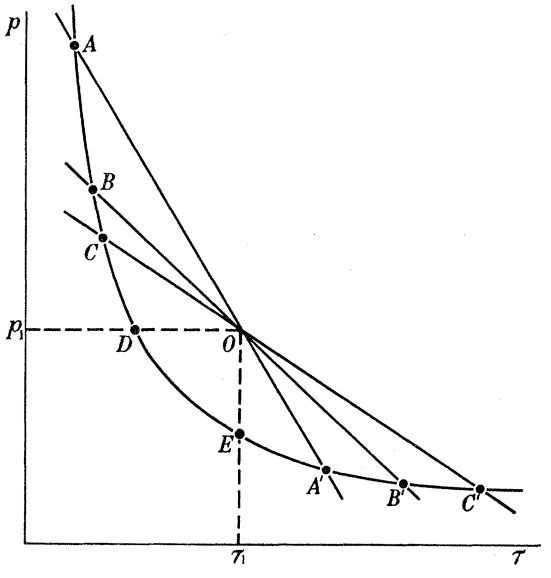

FIGURE 4. The Hugoniot diagram for case (c). The transitions are either strong R-type (OA, OB, OC) or strong D-type (OA', OB', OC'). A single transition line (BOB') is such that $v_1 = c_1$, and this separates those with $v_1 > c_1$ (AOA') from those with $v_1 < c_1$ (COC'). The limiting cases are the constant-pressure R-type (OD), and the constant-volume D-type (OE).

process is to reduce the total energy of the fluid, rather than to add to it. A further departure from the theory of combustion waves is that the Chapman–Jouguet hypothesis is certainly not valid for ionization fronts. In fact, the weak detonations and strong deflagrations which are forbidden by this hypothesis are analogous to weak R-type and strong D-type ionization fronts which are of fundamental importance in the theory of the propagation of ionization fronts.

It is important to distinguish between the Hugoniot curve used in this section and that usually used in discussing gas-dynamic discontinuities. Normally, the energy equation is used to obtain the Hugoniot function, but as this is in the form of a differential equation for ionization fronts it is more convenient to make use of the isothermal condition of the H II region and have a single Hugoniot curve for all cases instead of a different curve for each set of upstream conditions. The more conventional Hugoniot function does prove useful in discussing the structure of ionization fronts, as will be seen in § 5. In recognition of this

difference in the Hugoniot curves, the transitions represented by tangency of the transition line (2·3) to the Hugoniot curve (2·6), is called 'critical' rather than 'Chapman–Jouguet' as is usually the case.

3. The equations of the ionization front structure

It is assumed in deriving the equations of the ionization front structure, that the transition regions in which the gas changes from the practically unionized state of the H I region to the almost fully ionized state of the H II region, is thin. That is

(*a*) the thickness of the ionization front is small compared with the radius of the H II region, and

(*b*) in an unsteady case, the representative time for a change in the flow pattern is large compared with Δ/U_i, where Δ is the width of the ionization front and U_i is its velocity.

It is also assumed that shock waves are discontinuities of higher order than ionization fronts, and hence that they may be considered as discontinuities if they occur within the structure of the ionization front. The ratio of a typical length for the ionization process in the H I region (say, the mean free path of a photon) to the mean free path of hydrogen atoms in the H I region is $\sqrt{2}\,\pi\sigma^2/\alpha$, where σ is the Bohr diameter of a hydrogen atom. This has a value of about 10^2 which to some extent justifies the assumption.

With the use of the first assumption, the flow can be regarded as plane and quasi-steady, thus the operator $\mathrm{D}/\mathrm{D}t$ can be replaced by

$$\frac{\mathrm{D}}{\mathrm{D}t} = (u-U_i)\frac{\mathrm{d}}{\mathrm{d}r} = v\frac{\mathrm{d}}{\mathrm{d}r}, \tag{3·1}$$

giving, in the usual way, integrable forms for equations (1·5) and (1·4), which imply

$$\rho(u-U_i) = \rho v = m, \tag{3·2}$$

$$p+\rho(u-U_i)^2 = p+\rho v^2 = P, \tag{3·3}$$

where m and P are constant across the ionization front. It is convenient at this stage to introduce non-dimensional variables as follows:

$$\left.\begin{aligned} \rho &= \rho_0\bar{\rho}, \\ u &= U_i\bar{u}, \\ m &= -\rho_0 U_i A, \\ T &= T_c\theta, \\ P &= \rho_0 U_i^2 AB, \\ v &= U_i\bar{v}, \end{aligned}\right\} \tag{3·4}$$

where A and B depend on upstream conditions. In terms of these variables, equations (3·2) and (3·3) can be expressed as

$$\bar{v} = \tfrac{1}{2}B[-1+e\sqrt{(1-Y)}], \tag{3·5}$$

$$\bar{u} = 1+\bar{v}, \tag{3·5a}$$

$$\bar{w} = 3+2\bar{v}/B = 2+e\sqrt{(1-Y)}, \tag{3·5b}$$

$$\bar{\rho} = \frac{2A}{B}\left[\frac{1+e\sqrt{(1-Y)}}{Y}\right], \tag{3·6}$$

where $e = \mp 1$,
$$Y = \frac{2(1+x)\,\theta}{(U_i B/c)^2} = D(1+x)\,\theta, \tag{3·7}$$
$$c^2 = 2kT_c/M \quad \text{and} \quad D = 2(c/BU_i)^2.$$

The left-hand side of the energy equation (1·6) can be written
$$m\frac{\mathrm{d}}{\mathrm{d}r}\left(\frac{5p}{2\rho}+\frac{v^2}{2}\right);$$
if we put
$$\frac{5p}{2\rho}+\frac{v^2}{2} = \frac{U_i^2 B^2}{4}G, \tag{3·8}$$
it can be shown that
$$G = 1+2Y-e\sqrt{(1-Y)}, \tag{3·9a}$$
or
$$Y = \tfrac{1}{8}[4G-5+d\sqrt{(25-8G)}], \tag{3·9b}$$
where $d = \mp 1$.

With the substitution
$$j = -MJ/m, \tag{3·10}$$
equation (1·1) can be written
$$\frac{\mathrm{d}j}{\mathrm{d}r} = -\frac{\alpha\rho_0}{M}j\bar{\rho}(1-x). \tag{3·11}$$

Note that j is the ratio of the number of photons crossing unit area per second to the number of atoms crossing unit area per second from the H I region. This can be used to eliminate the terms involving $J\rho(1-x)$ on the right-hand side of equations (1·2) and (1·6). It is convenient to use j as independent variable, and with the aid of equation (3·11), equations (1·2) and (1·6) can be written
$$\frac{\mathrm{d}}{\mathrm{d}j}(j-x) = E\frac{x^2}{j(1-x)\,\theta^{\frac{3}{4}}}\frac{\bar{\rho}}{A}, \tag{3·12}$$
$$\frac{\mathrm{d}G}{\mathrm{d}j} = D\frac{T_*}{T_c}\frac{\mathrm{d}x}{\mathrm{d}j}+DH(\theta)\frac{\mathrm{d}}{\mathrm{d}j}(j-x), \tag{3·13}$$
where
$$E = \frac{\beta_0 c}{\alpha U_i T_c^{\frac{5}{4}}}\sqrt{\frac{M}{2k}}, \tag{3·14}$$
and
$$H(\theta) = \frac{T_*}{T_c}-\frac{3\theta}{2} \quad \text{when} \quad \theta < \frac{4000}{T_c},$$
otherwise,
$$H(\theta) = \frac{T_*}{T_c}-\frac{3\theta}{2}-\frac{0{\cdot}97\times 10^{-31}}{\beta_0 k}T_c^{\frac{7}{4}}\theta^{\frac{3}{4}}\left(\theta-\frac{4000}{T_c}\right)^2 \tag{3·15}$$

These two ordinary differential equations for G and x can be integrated from the upstream conditions $x = 0$ and $G = G_1$ at $j = 0$, if T_*, U_i and B (or D) are specified. The values of G and x at any point having been found, equation (3·9b) gives the value of Y, from which $\bar{v}$, $\bar{u}$, $\bar{w}$, $\bar{\rho}/A$, and θ can be calculated using (3·5), (3·6) and (3·7), respectively. Note that the value of A does not need to be specified in solving these equations since the factor $\bar{\rho}/A$ occurring in (3·12) is a function of B and Y only, as shown in equation (3·6).

The variation of r with j can be found by integrating equation (3·11), written in the form
$$\frac{\mathrm{d}\phi}{\mathrm{d}j} = \frac{1}{j(1-x)\,\bar{\rho}/A}, \tag{3·16}$$
where
$$\phi = \frac{\alpha\rho_0 A}{M}(r_i-r). \tag{3·17}$$

Since the ionization front has been assumed thin, the boundary condition for this equation is arbitrary, and in the calculations which follow in § 4, this condition is taken to be $\phi = 0$ when $j = 0{\cdot}10$.

It is an interesting feature of equation (3·16) that $\rho_0 A$ appears only as a scaling factor. This proves very useful when the results obtained here for the structure of an ionization front are linked with the external flow solution described by Goldsworthy. As ρ_0 is then taken to be $\omega_0/r_i^{\frac{1}{2}(n+1)}$, there is no need to calculate the value of ω_0 in order to discuss the structure. The relationships between the other variables used by Goldsworthy, and those used here are

$$\bar{u} = \mathscr{U}, \quad U_i/c = 1/\eta_i = \psi_i,$$
$$\bar{\rho} = \omega, \quad Y = 4\mathscr{A}^2/B^2.$$

In defining the speed of sound, it must be remembered that ahead of the ionization front, the gas is assumed to be perfect, with constant specific heats, whereas the gas behind the ionization front is isothermal. Thus it is necessary to define two Mach numbers, M_1 and M_2, such that

$$M_1^2 = \frac{(u-U_i)^2}{(\frac{5}{3}k/M)\,(1+x)\,T} = \frac{6}{5}\frac{U_i^2}{c^2}\frac{\bar{v}^2}{(1+x)\,\theta}, \tag{3·18a}$$

$$M_2^2 = \frac{(u-U_i)^2}{(k/M)\,(1+x)\,T} = \frac{2U_i^2}{c^2}\frac{\bar{v}^2}{(1+x)\,\theta}, \tag{3·18b}$$

being typical of the H I region, and the H II region, respectively. When equations (3·5) and (3·7) are substituted, (3·18) becomes

$$M_2 = Y^{-\frac{1}{2}}[1 - e\sqrt{(1-Y)}] = \sqrt{\tfrac{5}{3}}\,M_1. \tag{3·19}$$

Important conclusions can be drawn from the graph of G against Y. This is a parabola which touches the lines $Y = 1$ and $G = 25/8$ as shown in figure 5, where there is also drawn the parabola $\bar{w}(Y)$. Values of M_1 and M_2 and the corresponding signs of d and e are also indicated. The curve $G(Y)$ is closely related to the Rayleigh line in the theory of one-dimensional flow with heat addition.† If the motion of the ionization front is supersonic relative to the fluid ahead, M_1 must be initially greater than unity; figure 5 then shows that $d = e = -1$ in the initial part of the structure. On the other hand, if the ionization front moves subsonically relative to the fluid ahead, the integration must begin with $d = +1$, and e can take the values ± 1. At the rear of the structure, if the motion is to be subsonic relative to the fluid behind, M_2 must be less than unity, and the integration must therefore end with $d = e = +1$, while, if the motion relative to the fluid behind is supersonic, the integration must end with $e = -1$.

Equations (3·2) and (3·3), from which the expressions (3·5) and (3·6) are derived, represent the mechanical shock conditions. The third shock condition, representing conservation of energy, can be seen from (3·8) to be simply that G is constant across the shock. Hence, if the Mach number M_1 is greater than unity at some point in the ionization front, a shock can be inserted by manipulating d and e, keeping G, j and x constant. The latter assumptions require the shock wave to be of negligible thickness compared to the width of the ionization front. On the $G(Y)$ diagram, shocks are represented by lines of constant G, drawn from one side of the curve to the other, in the direction of increasing Y, since θ must

† Crocco (1958) and Saunders (1953).

increase through the shock. Thus, to insert a shock at a point at which $G < 3$, both d and e should be changed from -1 to $+1$, and if the shock is to be inserted at a point for which $G > 3$, only d is changed from -1 to $+1$ and e is left as -1.

It is constructive to consider first the case in which recombination and cooling by the excitation of oxygen ions is neglected. The propagation of ionization fronts of this type has been discussed by Kahn (1954) and Goldsworthy (1960). Since T_c has no meaning in this case, it should be replaced by T_*, and the structure equations are obtained by putting β_0 equal to zero and $H(\theta) = 1$. Equations (3·12) and (3·13) can then be integrated to give

$$\left.\begin{aligned} j &= x, \\ G &= Dx = Dj. \end{aligned}\right\} \tag{3·20}$$

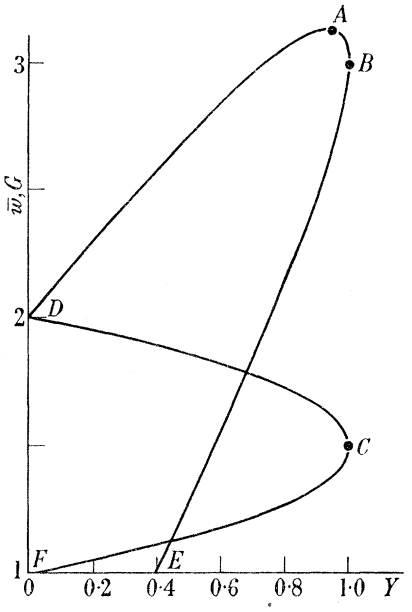

FIGURE 5. The invariant curves $\bar{w}(Y)$ and $G(Y)$. The parameter d is positive on EBA and negative on AD, changing sign at A. The parameter e is positive on EB and DC, changes sign at B and C, and is negative in BAD and CF; this determines corresponding points on the two curves. The Mach number M_1 decreases uniformly along $G(Y)$ in the direction $DABE$, being exactly unity at A. M_2 behaves in a similar manner, being unity at B.

Thus G is an increasing linear function of j throughout the structure, and the structure ends when j is equal to unity. From the Hugoniot diagram for this type of transition, it is easy to show that all R-type ionization fronts move supersonically relative to the fluid ahead, and all D-type ionization fronts move subsonically relative to the fluid ahead. The motion relative to the fluid downstream for the various types of ionization front is as found in § 2 except that the ordinary velocity of sound is used rather than the isothermal velocity of sound. Since G is a monotonic increasing function of j and since j increases across the structure, G will therefore have no turning value. Thus it is clear from figure 5 that an ionization front for which the relative motion is initially subsonic, must remain in this state. If the relative motion is initially supersonic then it will remain so, unless a shock is inserted. This causes the relative motion behind the shock to become subsonic. The former condition implies that a strong D-type transition is impossible for ionization fronts in which

recombination and cooling are absent. For other types of transitions, the condition $G \leqslant 25/8$ must be satisfied so that Y remains real. This puts a lower bound on the ionization front speed in some cases. For example, if the value of θ can be assumed to be negligible ahead of an R-type transition, then it can be shown that

$$U_i > 0{\cdot}75\sqrt{\frac{2kT_*}{M}}.$$

The value of U_i obtained by Goldsworthy for strong R-type transitions, easily satisfies the above inequality. However, as strong D-type transitions have been shown to be impossible in this case, the difficulty of determining the flow pattern when $\omega_0 < MJ_* R_*^2/2\sqrt{(kT_*/M)}$ still remains.

Consider now the structure of an ionization front, with the effects of cooling and recombination included. In the initial part of the structure these effects are small, since they are $O(x^2)$, and, in fact, calculations show that the equations (3·20) describe the structure adequately, even as far as about $x = 0{\cdot}7$. This is due to the small value of the coefficient E on the right-hand side of equation (3·12). For large values of j, the factor $(1-x)$ in this equation has an increasingly important effect, and eventually causes $\mathrm{d}x/\mathrm{d}j$ to tend asymptotically to zero. Equation (3·13) shows that $\mathrm{d}G/\mathrm{d}j$ also tends to zero asymptotically for large values of j. Generally, G is found to have a maximum somewhere near $j = 1$. If the maximum value of G is 25/8 exactly, a smooth changeover from supersonic to subsonic relative motion (and vice versa) in the ionization front structure is possible. This property is made use of in § 4 to show that flows may contain two shocks, one shock, or no shock at all, in contrast with the strictly one-shock patterns which must occur when recombination and cooling are neglected.

4. The solution of ionization front structures

The qualitative behaviour of ionization front structures can be understood most easily by reference to a diagram in which the quantities G and $\overline{w}$ are plotted as functions of Y and j. A typical diagram of this type is sketched in figure 6. The left-hand side of this diagram, in which the abscissa is Y, consists of two fixed curves, one given by (3·9a) and the other by (3·5b). The reader will note that these curves have already been given in figure 5, and are invariant to the type of ionization front. The right-hand side of the diagram varies from case to case, but it is sufficient for qualitative discussion to assume that $G(j)$ has the form suggested in § 3. That is, the slope of the curve is almost constant for small values of j, but decreases as the effects of recombination and cooling become more pronounced. In general, the curve has a turning point at which $G = G_{\max.} \leqslant 3\frac{1}{8}$. Beyond this point, G decreases rapidly at first, but as equilibrium is approached, $\mathrm{d}G/\mathrm{d}j \to 0$ slowly, and the curve tends asymptotically to the straight line $G = G(\infty)$. Only for very weak D-type ionization fronts will the general shape of the $G(j)$ curves differ, for instance, G may approach $G(\infty)$ from below, with $\mathrm{d}G/\mathrm{d}j \geqslant 0$ everywhere; this presents no difficulty. There is a one–one correspondence between points on the curves $G(j)$, $G(Y)$ and $\overline{w}(Y)$, which allows $\overline{w}(j)$ to be plotted to complete the diagram.

In addition to the qualitative discussion given in this section, the results of computed ionization front structures are shown for the more important cases. The computations were

carried out on the Manchester University electronic computer, which employs the four-step Runge–Kutta procedure in its integrating routine. Solutions were obtained for the range $0 \leqslant j \leqslant 4$, with a step length of 0·01, for several examples of each type of ionization front, and for values of T_* corresponding to stars of spectral type ranging from $O5$ to $B2$. The results are generally satisfactory, although in the cases for which G is required to have a maximum value of $3\frac{1}{8}$ so that the sign of d may be changed, they are slightly uneven due to the difficulty of adjusting the initial conditions to make $G_{\max.} = 3\frac{1}{8}$ exactly. For values of j greater than about 3, asymptotic solutions of the differential equations are found to be sufficiently accurate for most purposes.

It has been noted in § 3 that for a given type of ionization front and a given value of T_*, three other parameters, namely B, U_i/c and G_1, must be specified before the integrations can be carried out. There is some simplification for R-type ionization fronts if the temperature of the undisturbed H I region ahead is negligible compared with T_c, for then $A = B = 0$, $G_1 = 2$ and only U_i/c can vary. However, for D-type ionization fronts, all three parameters must be specified. To reduce the labour involved, only those D-type ionization fronts which occur in Goldsworthy's cylindrical problem are examined, and in this way, the number of independent parameters is once again reduced to one. The particular points at which weak D-type ionization front structures have been found are indicated on the integral curves in figure 1 as a, b, c and d.

4·1. *Weak D-type ionization fronts*

For weak D-type ionization fronts, the motion relative to the fluid ahead and behind is subsonic. Hence the solution for the structure must begin with $M_1 < 1$ and end with $M_2 < 1$. It is found that $G_{\max.}$ increases monotonically with U_i/c for given T_*, and as $G_{\max.}$ cannot exceed $3\frac{1}{8}$, there is a maximum value of U_i/c, say S, above which D-type structures are not possible. A typical case for which $U_i < cS$ is shown on the right-hand side of figure 6. Note that if $G_{\max.} < 3$ (as shown in figure 6), $e = +1$ and $M_2 < 1$ everywhere, but if $G_{\max.} > 3$, the sign of e must be changed as G passes through the value 3, and the structure therefore has a section in which $M_2 > 1$. The function $\overline{w}(j)$, which varies linearly with the fluid velocity, can be obtained most easily by using the left-hand side of figure 6. From the value of G, say point A, the value of Y can be found from the left-hand side of the figure, namely the point B. This determines the value of $\overline{w}$ at C and hence enables the point D to be plotted. It is important to note that the value of e is the same for corresponding points B and C, and in the case illustrated $d = e = +1$ throughout. The computed structure of a weak D-type ionization front, corresponding to the point (b) in figure 1, is shown in figures 7 and 8.

The limiting case of a weak D-type ionization front occurs when $U_i = cS$. This allows the possibility of a shock in the structure, for $G_{\max.} = 3\frac{1}{8}$ in this case, which enables the sign of d to be changed from plus to minus at the turning value, where the fluid speed and adiabatic sound speed are equal. The flow then becomes fully supersonic with $M_2 > M_1 \geqslant 1$. However, the relative motion must eventually become subsonic with $M_2 < 1$ so that a shock must occur at some stage after the point at which $G = 3\frac{1}{8}$ is reached. This type of structure is illustrated in figure 9, where corresponding points are joined by broken lines. Since the stagnation enthalpy is continuous at the shock, G must be continuous, and the transition is simply B to B'. The shock is made apparent on the right-hand side of the diagram by

the discontinuity in $\bar{w}$, namely DD'. This shock is of zero strength if introduced immediately when $G = G_{\max.}$ and if introduced at a later stage, the strength increases towards a limiting value. The position of the shock is arbitrary, which may at first seem alarming as it makes the structure not unique. However, it simply means that the different shock positions represent flows which do not differ sufficiently to be resolved by this approximate method of solution.

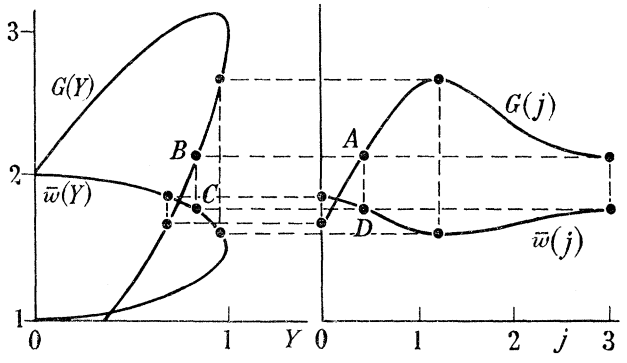

FIGURE 6. A sketch of the curves $(G, \bar{w})/(Y, j)$ for a typical weak D-type ionization front structure.

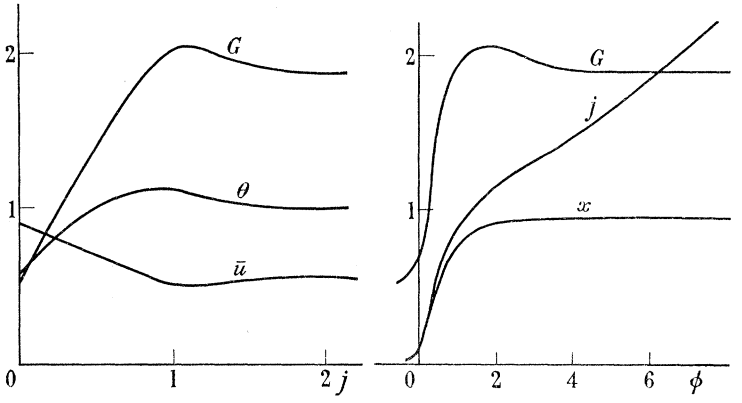

FIGURE 7 FIGURE 8

FIGURE 7. Profiles of G, θ and $\bar{u}$ against j for the structure of the weak D-type ionization front corresponding to the point (b) on figure 1; $T_* = 40\,000\,°\mathrm{K}$.

FIGURE 8. G, j and x as functions of ϕ for the weak D-type ionization front structure of figure 7.

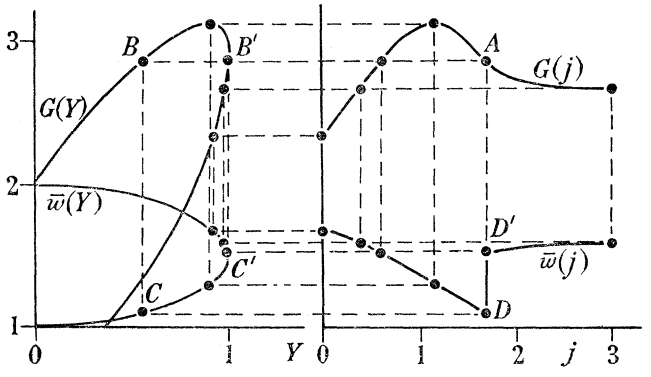

FIGURE 9. A sketch of the curves $(G, \bar{w})/(Y, j)$ for the limiting case of a weak D-type ionization front structure. The shock, which is shown here at $j = 1{\cdot}7$, can be inserted arbitrarily at any point after G has its maximum value of $3\frac{1}{8}$.

In figure 10, the velocity distribution in a weak D-type ionization front is shown plotted as a function of j for three different values of U_i/c. As U_i/c is increased, the dip in the profile can be seen to become more and more pronounced, and eventually a shock is formed. This behaviour is similar to the steepening of an ordinary compression wave, and it illustrates the formation of the isothermal shock which follows a strong D-type ionization front.

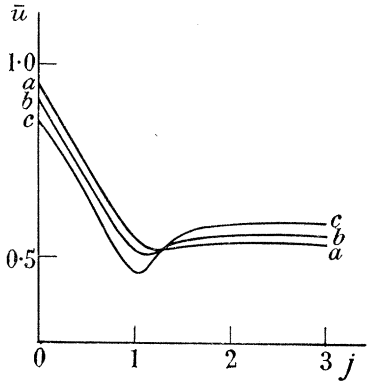

FIGURE 10. Non-dimensional velocity profiles in weak D-type ionization front structures corresponding to the points (a), (b) and (c) on figure 1; $T_* = 40\,000\,°\mathrm{K}$. The dip in the velocity profile eventually produces a shock in the limiting case. This occurs at a point between (c) and (d) on figure 1 (see C'' on figure 21).

4·2. *Weak R-type ionization fronts*

For weak R-type ionization fronts, the motion relative to the fluid ahead and behind is supersonic, that is, $M_1 > 1$ ahead, and $M_2 > 1$ behind. The solution for the structure must therefore begin with $d = -1$ and end with $e = -1$. Computations show that $G_{\max.} < 3\frac{1}{8}$ for all U_i/c greater than a certain value, say S'. In such a case, M_1 and M_2 are greater than

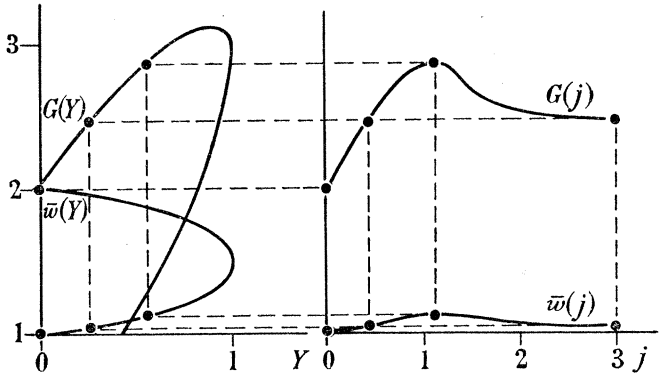

FIGURE 11. A sketch of the curves $(G, \bar{w})/(Y, j)$ for a typical shockless weak R-type ionization front structure.

unity throughout the structure, and the relative motion is supersonic everywhere. The $(G, \bar{w})/(Y, j)$ diagram for an ionization front of this type is shown in figure 11. Computed results are shown in figures 12 and 13 for an example in which $U_i/c = 3{\cdot}16$ and $T_* = 40\,000\,°\mathrm{K}$.

A more complex weak R-type structure is possible when $U_i/c < S'$ for in this case a shock must be inserted at some point before $G = G_{\max.}$. The effect of this shock is to reduce the

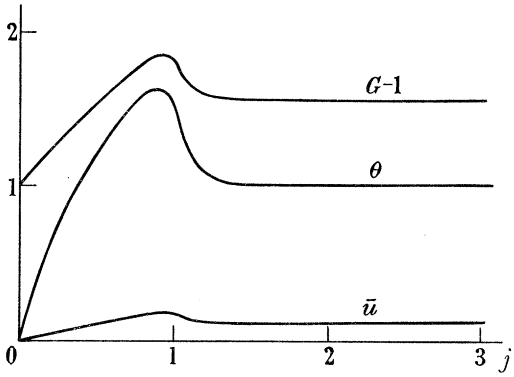

FIGURE 12

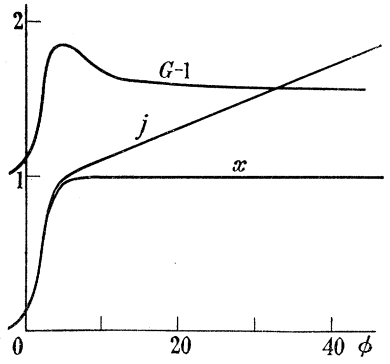

FIGURE 13

FIGURE 12. Profiles of $(G-1)$, θ and $\bar{u}$ against j for a weak R-type ionization structure corresponding to the point $\psi = 3{\cdot}16$ on the curve D in figure 1; $T_* = 40\,000\,^\circ\mathrm{K}$.

FIGURE 13. $(G-1)$, j and x as functions of ϕ for the weak R-type ionization front structure of figure 12.

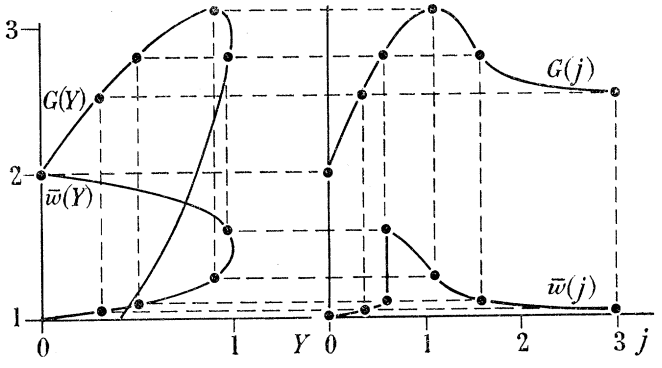

FIGURE 14. A sketch of the curves $(G, \bar{w})/(Y, j)$ for the case of a weak R-type ionization front containing a shock.

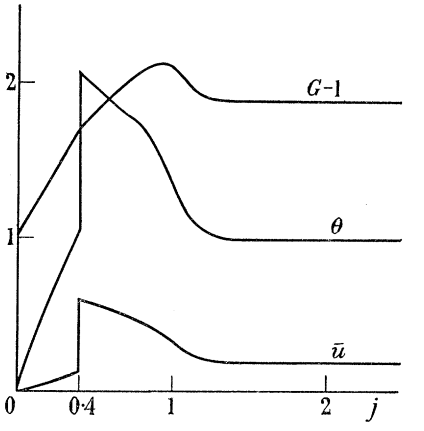

FIGURE 15

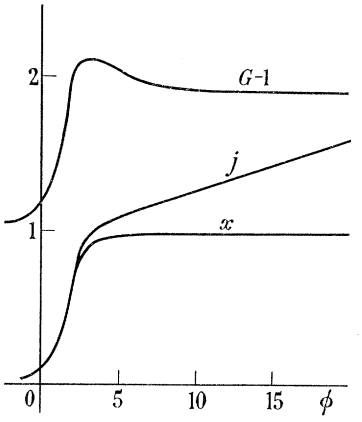

FIGURE 16

FIGURE 15. Profiles of $(G-1)$, θ and $\bar{u}$ against j, for a weak R-type ionization front structure containing a shock at $j = 0{\cdot}4$; $T_* = 40\,000\,^\circ\mathrm{K}$. This ionization front occurs at the point $\psi = 2{\cdot}46$ on the curve D in figure 1.

FIGURE 16. $(G-1)$, j and x as functions of ϕ for the weak R-type ionization front structure of figure 15.

value of $G_{\max.}$ for the given value of U_i/c, and thus if $U_i/c < S'$ it is possible to find a unique shock position which makes $G_{\max.} = 3\frac{1}{8}$. In this way the relative motion is made subsonic in a short section behind the shock, and the condition that $M_2 > 1$ at the rear of the structure can be satisfied by changing the sign of d when $G = 3\frac{1}{8}$, if necessary. This case is depicted in figure 14, and a computed example is shown in figures 15 and 16 for a case in which the shock appears at $j = 0{\cdot}40$, and $T_* = 40\,000\,^\circ\mathrm{K}$. The discontinuity in $\mathrm{d}G/\mathrm{d}j$ to be seen in figure 15 shows the effect of the shock in reducing the value of $G_{\max.}$. This is the result of increasing the temperature so that $H(\theta)$ becomes large and negative, and hence $\mathrm{d}G/\mathrm{d}j$ is reduced immediately (see (3·13)).

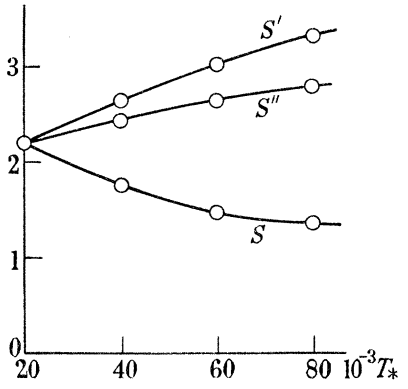

FIGURE 17. The variation of S, S' and S'' with T_*. The curve S as shown, refers only to the cylindrical problem but may be regarded as being a typical example of its class; the curves S' and S'' are universal.

In order to find weak R-type structures for successively smaller values of U_i/c (below S') it is necessary to move the shock forward in the structure. There is a limiting case when $U_i/c = S''$ say, for which the shock is at $j = 0$, and thus weak R-type ionization fronts are not possible with $U_i < cS''$. The variation of S, S' and S'' with T_* is shown in figure 17. Clearly, if $T_* > 20\,000\,^\circ\mathrm{K}$, there is always a range of values of U_i/c lying between S and S'', in which neither a weak R-type nor a weak D-type ionization front is possible, and this gap must be filled by strong D-type ionization fronts.

4·3. *Strong D-type ionization fronts*

A strong D-type ionization front moves subsonically relative to the fluid ahead, and supersonically relative to the fluid behind. Therefore the solution for the structure must begin with $e = d = +1$ and end with $e = -1$, and usually with $d = -1$. This can be possible only if $G_{\max.} = 3\frac{1}{8}$ exactly, and so structures can be found only for certain combinations of the parameters T_*, B, G_1, and U_i/c. There are, in fact, only three degrees of freedom in the choice of these four parameters. The $(G, \overline{w})/(Y, j)$ diagram for a strong D-type ionization front structure is shown in figure 18 and the results for a computed example are shown in figures 19 and 20.

It is interesting to note that the one degree of indeterminancy of strong D-type ionization fronts found in Goldsworthy's solution is balanced by the extra condition requiring that $G_{\max.} = 3\frac{1}{8}$ in the structure. That is, if conditions ahead of the ionization front are given by

a point on the 'strong shock' curve in figure 1 (thus providing two relations between B, G_1 and U_i/c), then for a given value of T_* there is at most one value of U_i/c at which a real ionization front structure exists. Hence the combination of solutions for the ionization front structures and for the flow in the large gives a unique solution to the problem of the propagation of an ionization front. The strong D-type ionization fronts which are permissible in Goldsworthy's cylindrical problem are indicated in figure 21. Note that when

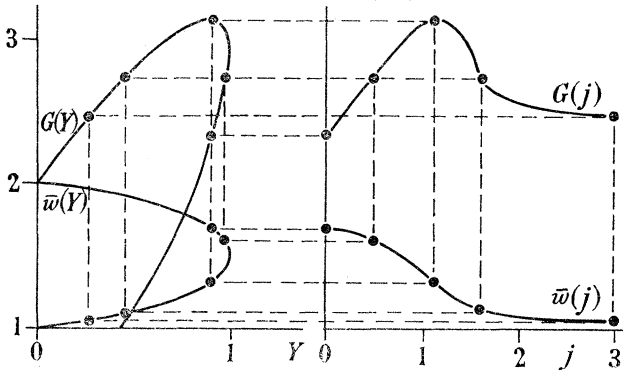

FIGURE 18. A sketch of the curves $(G, \bar{w})/(Y, j)$ for a typical strong D-type ionization front structure.

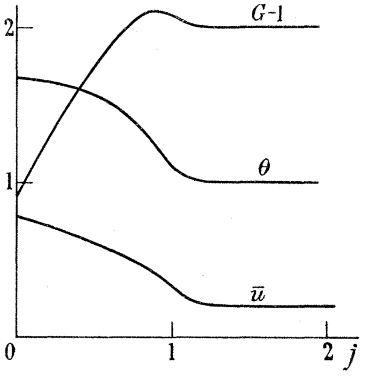

FIGURE 19

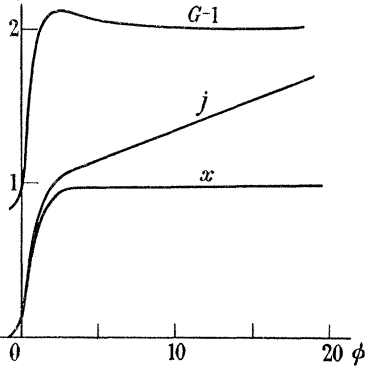

FIGURE 20

FIGURE 19. Profiles of $(G-1)$, θ and $\bar{u}$ against j, for a strong D-type ionization front structure corresponding to the point P on figure 21; $T_* = 40\,000\,^\circ\mathrm{K}$.

FIGURE 20. $(G-1)$, j and x as functions of ϕ for the strong D-type ionization front structure of figure 19.

$T_* = 20\,000\,^\circ\mathrm{K}$, no strong D-type flow patterns are possible, and the link between the weak R-type and weak D-type flow patterns is a single strong R-type pattern rather than a range of strong D-types. For $T_* > 20\,000\,^\circ\mathrm{K}$, there is always a range of possible strong D-types, which increases for larger values of T_*. The strong R-type flow pattern is not possible if $T_* > 20\,000\,^\circ\mathrm{K}$.

One limiting case of the strong D-type structure occurs when the ionization front combines with the leading shock so that there is no disturbance in the H I region. This is the same as the limiting case of the weak R-type structure. A second limiting case occurs when the trailing isothermal shock coincides with the ionization front, and this is the same as the limiting case of a weak D-type structure.

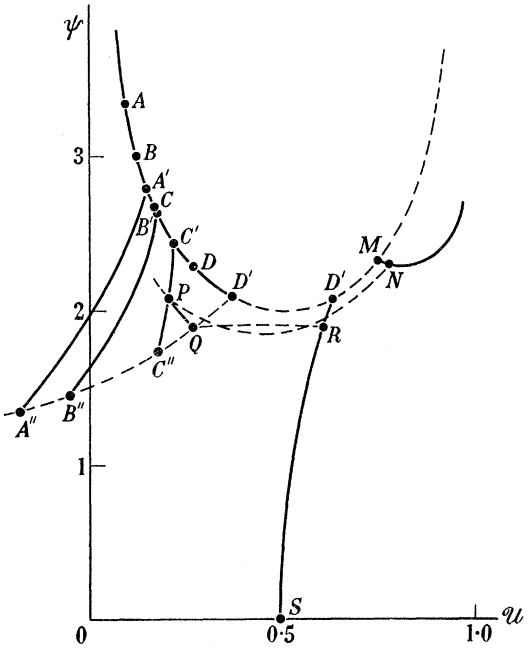

FIGURE 21. Loci of unique solutions for the cylindrical problem. For the curve $T_* = 80\,000\,°\mathrm{K}$, shockless weak R-type ionization fronts occur above the point A on the R-type locus; in AA', the ionization front is weak R-type but contains a shock. The locus of possible strong D-type ionization fronts is shown as $A'A''$, and ionization fronts with a smaller value of U_i/c than that at A'' are weak D-type. The corresponding curves for the cases $T_* = 60\,000\,°\mathrm{K}$, $40\,000\,°\mathrm{K}$ and $20\,000\,°\mathrm{K}$ are shown as $BB'B''$, $CC'C''$ and $DD'D''$, respectively. Note that no strong D-types are possible when $T_* = 20\,000\,°\mathrm{K}$.

The complete external solution for the strong D-type ionization front of figures 19 and 20 is indicated. SR represents the flow in the first H II region, RQ the isothermal shock, QP the flow in the second H II region, PN the ionization front, NM the flow in the H I region, and M the strong shock.

4·4. *Strong R-type ionization fronts*

The strong R-type ionization front may be regarded as being rather a special case as it requires that the leading shock in the H I region and the trailing isothermal shock in the H II region should both coincide with the ionization front. In the cylindrical problem there is only one value of U_i/c at which this can happen, and then only if T_* is not greater than $20\,000\,°\mathrm{K}$.

Since the motion relative to the fluid ahead and behind is supersonic and subsonic, respectively, the solution for the structure of a strong R-type ionization front must begin with $e = d = -1$ and end with $e = d = +1$. For a certain set of values of the parameters T_*, B, U_i/c and G_1, a solution which does not contain a shock is possible. This requires that $G_{\max.} = 3\frac{1}{8}$ so that if $G_1 = 2$, and B is taken to be zero, a structure of this type can be found only if a certain relationship between U_i/c and T_* is satisfied. In the cylindrical problem, U_i/c has a fixed value and a shockless strong R-type structure is possible for only one value of T_*. The $(G, \overline{w})/(Y, j)$ diagram for this case is shown in figure 22.

A strong R-type ionization front structure with one shock is the one which is most likely to occur. This single shock can be inserted anywhere in the structure, provided $G_{\max.} \leqslant 3\frac{1}{8}$. If a shock is inserted at a suitable point in the initial part of the structure, it may be possible

to make $G_{\max.} = 3\frac{1}{8}$ so that a change back to supersonic conditions is possible. In such a case a second shock must be inserted in the tail of the structure to make the relative motion subsonic as required. The position of this second shock is not unique, and in fact it corresponds to the shock occurring in the limiting weak D-type ionization front. The $(G, \bar{w})/(Y, j)$ diagrams for one-shock and two-shock strong R-type ionization fronts are shown in figures 23 and 24.

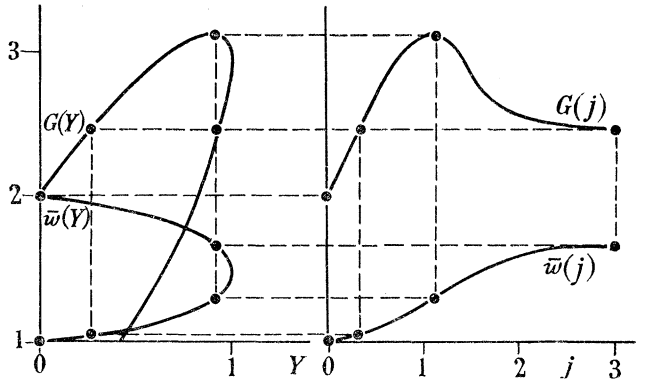

FIGURE 22. A sketch of the curves $(G, \bar{w})/(Y, j)$ for a strong R-type ionization front structure which does not contain a shock. Note that $G_{\max.} = 3\frac{1}{8}$.

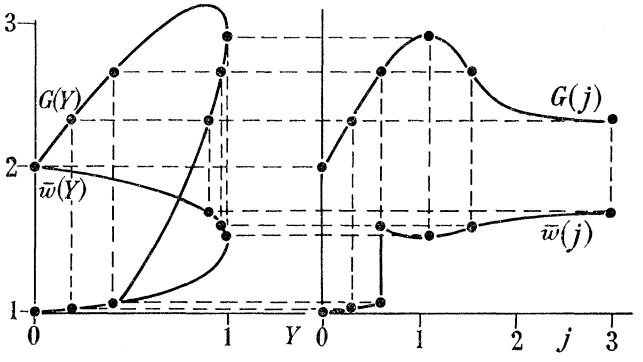

FIGURE 23. A sketch of the curves $(G, \bar{w})/(Y, j)$ for a strong R-type ionization structure which contains one shock. Note that $G_{\max.}$ does not have to be $3\frac{1}{8}$.

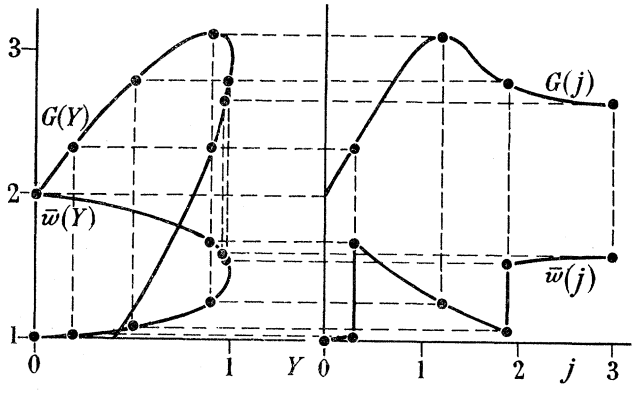

FIGURE 24. A sketch of the curves $(G, \bar{w})/(Y, j)$ for a strong R-type ionization front structure containing two shocks. Behind the first shock, G continues to increase until it reaches a maximum of $3\frac{1}{8}$ when the flow is sonic. By coming down the supersonic side of $G(Y)$, the insertion of a second shock is made possible.

4·5. *Application of results to the external flow*

Having found examples of all types of ionization front structures, it is possible to examine the validity of some of the assumptions listed in § 1. These have been discussed by Goldsworthy, but in several cases further information is needed from the structure solutions before any definite conclusions can be reached. In other cases, the structure solutions give added support.

The computed results show that the gas, having passed through the ionization front, is almost fully ionized and at the equilibrium temperature T_c. This condition is reached in all cases for values of j from about 2 onwards. Thus the rate at which photons reach the 'back' of the ionization front is no more than about twice the rate at which ionized atoms enter the ionization front from the H I region. Hence the condition for the validity of the assumption that $J_i r_i^n \ll J_* R_*^n$ can be written

$$\frac{2\rho_0(r_i)\, U_i A r_i^n}{M J_* R_*^n} \ll 1. \tag{4·1}$$

In Goldsworthy's similarity solutions, $\rho_0(r_i) = \omega_0 / r_i^{\frac{1}{2}(n+1)}$, and for the cylindrical case ($n = 1$), the condition reduces to

$$\frac{\omega_0 A U_i}{c} \ll \frac{J_* R_* M}{2c}. \tag{4·2}$$

Approximate solutions for extreme cases of weak R- and D-type ionization fronts show that the assumption breaks down for the fastest weak R-types. With the use of the expression

$$\omega_0^2 \approx \frac{M^2 T_c^{\frac{3}{4}} J_* R_*}{\beta_0 (3{\cdot}3 + \ln (U_i/c))}, \tag{4·3}$$

which is roughly correct for large values of U_i/c, the condition (4·2) can be written

$$U_i/c \ll (3 J_* R_* / 10^{25})^{\frac{1}{2}}. \tag{4·4}$$

The right-hand side of this inequality has values in the range 200 to 2×10^4 for stars of spectral type $B2$ to $O5$, and the assumption is therefore valid for all but the most tremendous ionization front speeds. In the spherical case however, $n = 2$, and the condition (4·1) will break down at some finite value of r_i, of order $(2MJ_* R_*^2 / A\omega_0 U_i)^2$ approximately.

The assumption that the ionization front is thin compared with a typical length, L, of the flow, can be expressed

$$\frac{\Delta}{L} \approx \frac{M\phi_i}{\alpha \rho_0 A L} \ll 1, \tag{4·5}$$

where ϕ_i is a value of ϕ at which equilibrium is reached in the ionization front structure. Computed results show that ϕ_i may be taken to be about 10, and if L is taken to be the radius of the H II region, r_i (centimetres), then for the similarity solutions

$$A\omega_0 \gg 6 \times 10^{-6} r_i^{-\frac{1}{2}(n-1)}. \tag{4·6}$$

In the cylindrical case the assumption is valid for all but the fastest weak R-type ionization fronts, corresponding to values of ω_0 less than about 10^{-5}. In the spherical case, the assumption may be regarded as being true in general.

The actual thickness of an ionization front varies greatly, but in most cases the expression for Δ used in (4·5) should give a reasonable estimate of the order of magnitude of the

thickness, if ϕ_i/A is taken to be about 10. Thus the equilibrium conditions of the H II region just downstream of the ionization front are reached in a distance of approximately 10^3 hydrogen atom mean free paths from the H I region. More conveniently, the width of the ionization front is given by

$$\Delta = O(1/2N) \text{ parsecs}, \tag{4·7}$$

where N is the number of hydrogen atoms per cubic centimetre in the H I region ahead of the ionization front.

The solution of equation (3·16) for small values of j is

$$j = x = j_1 \exp\left\{-\frac{\alpha\rho r_i}{M}\left(\frac{r-r_i}{r_i}\right)\right\}, \tag{4·8}$$

where j_1 is the point (arbitrarily chosen) in the ionization front structure at which $r = r_i$. This expression shows that the level of ionization in the early part of the structure decreases exponentially with constant $1/\alpha N r_i$. This constant is the ratio of the mean free path for absorption in the H I region to the radius of the H II region, and the decrease in j and x is therefore very rapid for all but very small values of Nr_i. Thus, the assumption that ionization and preheating of the H I region ahead of the ionization front can be neglected in the external flow solution appears to be reasonable in general.

The external flow solution could be improved slightly by allowing for cooling processes in the neutral gas. Hydrogen molecules provide the most likely mechanism for cooling in the H I regions (Kahn 1955), and their effects could be included simply by the addition of an extra term on the right of equation (1·6). This would have very little effect on the ionization front structures, but the integral curve for the flow in the H I region (shown in figure 1) may be altered considerably. Thus the loci of possible strong D-type ionization fronts would differ from those shown in figure 21, although the general character of the curves would remain unchanged.

5. The Chapman–Jouguet hypothesis

Since weak R-type ionization fronts correspond to weak detonations, and strong D-type ionization fronts correspond to strong deflagrations, it would be expected on the basis of the Chapman–Jouguet hypothesis, that such ionization fronts are not possible. Yet it has been clearly demonstrated (theoretically) in the preceding sections that weak R-type and strong D-type ionization fronts must occur. Hence there is a contradiction between the results obtained in this paper and the Chapman–Jouguet hypothesis, which requires explanation.

It has been suggested to the author that the reason that some ionization fronts can move supersonically relative to the fluid behind them is that the signals maintaining the strength of the front travel into it at the speed of light, since it is radiation that causes the ionization. For combustion waves, however, it is presumed that these signals cannot travel at more than the sound speed of the burnt gas behind the wave, since the combustion is caused by molecular collisions. Thus, the argument goes, weak detonations and strong deflagrations cannot occur since they require that the motion relative to the fluid behind is supersonic. With these ideas in mind, Taylor & Tankin (1958) have suggested that a weak detonation could be produced in a combustion process if it were maintained by an independent parallel detonation, which could be provided by detonating cord, or a series of spark plugs.†

† A similar idea has been put forward by Zel'dovich (1950).

There is an obvious analogy between this independent detonation and radiation, in the case of ionization fronts.

The 'signals' argument would be justified if ionization fronts were such that recombination and cooling could be neglected, for here the strong D-type ionization front has been proved impossible, and the weak R-type ionization fronts (which, incidentally, are shockless) can be said to occur only because the ionizing process is independent of any motion of the fluid. But what can be said in the case of ionization fronts with cooling and recombination included? Here strong D-type ionization fronts, and weak R-type ionization fronts with shocks in their structure, certainly occur, in addition to the shockless weak R-type, and it is not the ionizing mechanism but the presence of cooling and recombination which permits this. The necessary condition for the existence of these ionization fronts is that the function G (equation (3·8)), should have a turning value (maximum) at the point where it is exactly equal to $25/8$ and then decrease towards a value $G(\infty)$, $(< 25/8)$. That is, the cooling should be strong and most efficient when the processes involved are nearly complete, so that the total energy will have a maximum and then 'relax' towards some equilibrium value. For a wave having this property, the Chapman–Jouguet hypothesis cannot be deduced as a consequence of the 'signals' argument, as it cannot be argued that the speed of say, a combustion process is limited by the speed at which signals from the burnt gas can penetrate to the unburnt gas. The burnt gas in this case is in an equilibrium state and has a lower stagnation enthalpy than some of the gas ahead. Thus if the strength of the process is maintained by signals from the fluid which has the greatest stagnation enthalpy, the combustion zone can quite easily move supersonically relative to the fluid behind, as these signals are propagated at a speed greater than the equilibrium sound speed.

The 'signals' argument, as shown here, can be used to demonstrate that non-Chapman–Jouguet waves are possible under certain circumstances. No satisfactory picture of the structure of the wave can be found in this way, however, as there is no reason to believe that signals from downstream are all-important in determining the flow. The whole process has a more accurate analogy with one-dimensional flow in a constant area duct with heat exchange (Saunders 1953; Crocco 1958). The connexion between the Rayleigh line, which is important in the latter case, and the $G(Y)$ curve of this paper, has already been noted. When heat is added to the flow in such a channel, the Mach number becomes closer to unity whether the flow is supersonic or subsonic. When the Mach number is unity, no further addition of heat is possible without causing a breakdown of the flow. Exactly the same situation is found in ionization front structures when cooling and recombination are neglected and the process is therefore exothermic. Here the function G increases monotonically throughout the structure, and, as can be seen from figure 5, the Mach number M_1 approaches unity. No structures are possible if $G > 25/8$, and when $G = 25/8$ the Mach number is exactly unity. Shocks can be inserted in both the channel and the ionization front to alter the flow from supersonic to subsonic, but there is no mechanism whereby this change, or its reverse, can be made smoothly. Thus, if heat is always added to the flow in the channel, or if the process involved in the ionization front is purely exothermic, the Chapman–Jouguet hypothesis is obeyed. However, if heat is first added and then subtracted from the channel flow, or if the ionization front is exothermic and then endothermic, changes can be made quite smoothly in the Mach number at the value unity, as long as this point coincides

PHILOSOPHICAL TRANSACTIONS OF THE ROYAL SOCIETY A MATHEMATICAL, PHYSICAL & ENGINEERING SCIENCES

with the point at which the heat input to the flow is zero. In this case, the Chapman–Jouguet hypothesis need not be obeyed.

Arguments supporting the Chapman–Jouguet hypothesis are often given with the aid of the conventional Hugoniot diagram. However, these arguments always require that the wave in question is exothermic everywhere. If this condition is relaxed, the Hugoniot diagram proves an excellent means of demonstrating that non-Chapman–Jouguet waves can exist. Consider the transition relations

$$\rho v = m, \tag{5·1}$$

$$p+\rho v^2 = P, \tag{5·2}$$

$$\frac{\gamma}{\gamma-1}\frac{p}{\rho}+\tfrac{1}{2}v^2 = E_1+E(\epsilon), \tag{5·3}$$

where m, P, E_1, are constants depending on upstream conditions, and $E(\epsilon)$ is the energy added to the fluid per unit mass up to the point where a fraction ϵ of the fluid has been converted by the particular process involved. These equations apply to ionization fronts, combustion waves, and any similar gas-dynamic discontinuities: the terms 'detonation' and 'deflagration' will be used in the loose sense when referring to the conventional Hugoniot diagram, and will include R- and D-type ionization fronts. In the case of ionization fronts, ϵ is equivalent to x (the fraction of ionized atoms) and, apart from an added constant, $E(\epsilon)$ is proportional to G. For combustion waves, ϵ is the fraction of burnt gas. Writing

$$\tau = 1/\rho, \tag{5·4}$$

and eliminating v from (5·3), the Hugoniot relation is found to be

$$\frac{1}{\gamma-1}(p\tau-p_1\tau_1)+\tfrac{1}{2}(p+p_1)(\tau-\tau_1) = E(\epsilon). \tag{5·5}$$

As in § 2, there is a 'transition line' given by

$$p-p_1 = -m^2(\tau-\tau_1), \tag{5·6}$$

where the subscript 1 refers to conditions upstream of the wave. This is a straight line of negative slope from the point (p_1, τ_1) which must cut every one of the family of Hugoniot curves generated by taking all values of ϵ between 0 and 1, and if it does not do this no transition is possible. Also, ϵ must vary continuously along the transition line, unless there is a shock, when there is a jump to the second intersection of the transition line and the Hugoniot curve for the particular value of ϵ.† The jump in this case must be in the direction of increasing p. Details of the structure of a wave can be found by following the transition along the transition line, from the point (p_1, τ_1) which lies on the Hugoniot curve $\epsilon = 0$, until all the Hugoniot curves for $0 \leqslant \epsilon \leqslant 1$ have been traversed; in this way p and τ can immediately be plotted as functions of ϵ.

Up to this point, the analysis is the same as that given usually for combustion waves (see, for example, Courant & Friedrichs 1948) but here, instead of assuming that $E(\epsilon)$ is an increasing function of ϵ everywhere, it is assumed that it first increases from zero, reaches

† Each Hugoniot curve is, of course, the Hugoniot curve for a shock, since (5·1), (5·2) and (5·3), with ϵ constant, are the Rankine–Hugoniot relations.

a maximum, and then decreases towards an equilibrium value E_2. Thus, for a certain range of values of ϵ, $E(\epsilon)$ takes on the same values twice, and the Hugoniot curve $\mathscr{H}'$ lying furthest from the origin is not the one corresponding to $\epsilon = 1$ (as in Courant & Friedrichs' diagrams) but it is the curve corresponding to the value of ϵ (say ϵ') for which $E(\epsilon)$ is a maximum.†

The deflagration branch of a typical Hugoniot diagram is shown in figure 25. The initial conditions are given by the point O, and the three transition lines shown correspond to three different values of m. The transition line OA cannot give a real structure as it does not

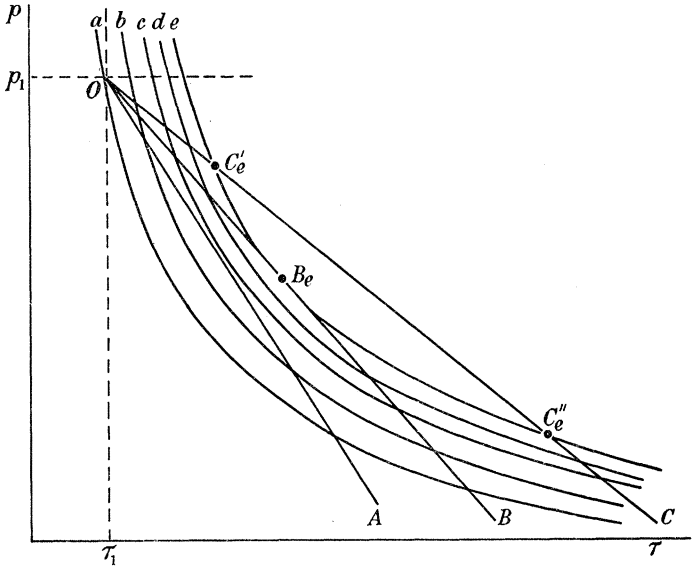

FIGURE 25. The deflagration branch of a Hugoniot diagram for a partly endothermic wave. Each Hugoniot curve corresponds to a different value of ϵ, curve (a) having $\epsilon = 0$, and curve (e) (which is $\mathscr{H}'$) having $\epsilon = \epsilon'$. Curves (b), (c) and (d) correspond to increasing values of ϵ in the range $0 < \epsilon < \epsilon'$, and (d) also serves as the final Hugoniot curve with $\epsilon = 1$. Points of intersection are denoted by an obvious notation (e.g. C''_b), single primes referring to the first, and double primes to the second intersection. A typical weak deflagration is $[O, C'_b, C'_c, C'_d(\epsilon < \epsilon'), C'_e, C'_d(\epsilon = 1)]$. The only possible strong deflagration is $[O, B'_b, B'_c, B'_d(\epsilon < \epsilon'), B_e, B''_d(\epsilon = 1)]$.

This set of curves can be used to give the result for purely exothermic waves that only weak deflagrations are possible, if (b), (c), (d) correspond to increasing values of ϵ in $0 < \epsilon < 1$, and (e) is the final curve with $\epsilon = 1$.

cut all the Hugoniot curves. Only a weak deflagration is allowed along the transition line OC, for the strong deflagration given by this line has a section $C'_e C''_e$ which corresponds to a rarefaction shock, and is therefore impossible. Note that the density decreases in the weak deflagration until $\epsilon = \epsilon'$ when it has a minimum, and it then increases until $\epsilon = 1$ at the rear of the structure. The pressure also has a minimum value. Only one of the infinity of possible transition lines drawn from O can give a strong deflagration, and this is the one which is a tangent to $\mathscr{H}'$. This transition may be regarded as having an 'internal' Chapman–

† This possibility has also been noted by Ya. B. Zel'dovich and S. B. Ratner, whose work is referred to by Landau & Lifshitz (1959, p. 485). However, their only conclusion seems to be that a detonation containing an internal Chapman–Jouguet point does not move at sonic speed relative to the gas downstream. The more important results, namely, that strong deflagrations and weak detonations (containing a shock) can exist in this case, and that strong deflagrations are internally overdetermined, have apparently escaped these writers.

Jouguet point, which has the same properties as an ordinary Chapman–Jouguet point, including that the fluid entropy is a maximum and the relative velocity is exactly sonic. The over-determined nature of the structure of a strong deflagration matches the under-determined state of the flow in the large, and together these should produce a unique solution in any given case. Note that the transition line which is tangential to $\mathscr{H}'$ gives possible weak deflagrations containing shocks which may be regarded as limiting cases (maximum value of m) of weak deflagrations for given (p_1, τ_1).

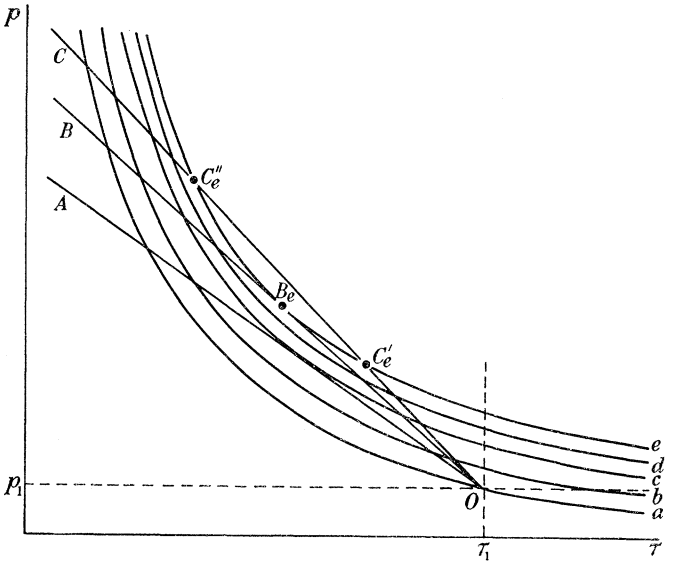

FIGURE 26. The detonation branch of a Hugoniot diagram for a partly endothermic wave (notation as in figure 25). A typical (shockless) weak detonation is $[O, C'_b, C'_c, C'_d(\epsilon < \epsilon'), C'_e, C'_d(\epsilon = 1)]$ and a typical strong detonation is $[O, C'_b, C'_c, C''_c, C''_d(\epsilon < \epsilon'), C''_e, C''_d(\epsilon = 1)]$, where the shock is on the Hugoniot curve (c). The transition line OB, containing the internal Chapman–Jouguet point B_e, permits a shocked weak detonation such as $[O, B'_b, B''_b, B''_c, B''_d(\epsilon < \epsilon'), B_e, B'_d(\epsilon = 1)]$; this line also permits strong detonations with no shock or two shocks, as well as the limiting forms of the more usual strong and weak detonations such as those occurring on OC.

In the form appropriate to purely exothermic waves (i.e. $\epsilon = 1$ on (e)), this diagram gives the result that only shockless weak detonations are possible, and strong detonations must contain a single shock.

Figure 26 shows the detonation branch of a Hugoniot diagram to be similar to the deflagration branch, except that more opportunity is available for the insertion of a shock. Normally strong detonations must contain a shock and weak detonations must be shockless. However, if the transition line is a tangent to $\mathscr{H}'$, strong detonations can be constructed having one shock, two shocks, or no shock at all. There is a single weak detonation which contains a shock, also lying on the transition line tangential to $\mathscr{H}'$. The strong detonations with a single shock may be regarded as being strong detonations as far as the shock, but thereafter, as weak deflagrations from a base point which is the second intersection of the transition line with the Hugoniot curve corresponding to $\epsilon = 0$. In the same way the single weak detonation with a shock can be regarded as being partly a strong deflagration. However, the ordinary shockless weak detonation has no deflagration-like region, and the argument, that weak detonations will not occur if it can be proved that strong deflagrations do not, is therefore unsound. Certainly, the weak detonations with shocks will not occur if

strong deflagrations are impossible, as has been shown for ionization fronts with cooling and recombination neglected. The weak detonations are therefore of two classes, those with a shock depending on the presence of cooling for their existence, and those without presumably requiring that their maintenance does not depend on signals being received from the gas downstream.

This description of the Hugoniot diagram for processes which are not exothermic everywhere, is similar to that given in § 4, in terms of $(G, \overline{w})/(Y, j)$ diagrams. However, the processes involved have not been specified, and the results are therefore true for any type of wave in which there are both exothermic and endothermic sections.

Some arguments in support of the Chapman–Jouguet hypothesis are based on entropy considerations. However, this approach is not likely to prove helpful. For instance, equation (5·3) can be written in differential form as follows,

$$\mathrm{d}E = \frac{\gamma}{\gamma - 1}\mathrm{d}\left(\frac{p}{\rho}\right) + \frac{m^2}{\rho}\mathrm{d}\left(\frac{1}{\rho}\right) = T\mathrm{d}S, \tag{5·7}$$

where S is the entropy of the fluid per unit mass. Thus the point at which E has a maximum is also a maximum for the fluid entropy. As remarked earlier, E is proportional to G, in the notation employed in previous sections, and bearing in mind the shape of computed curves for G in typical ionization front structures it is clear that there is a section in which the fluid entropy decreases in nearly every case. This does not violate the second law of thermodynamics however, as, in addition to the fluid entropy, the entropy of the radiation and the entropy associated with energy latent in excited particles must be considered. For ionization fronts, a rough analysis can be made which shows that the total entropy increases in the direction of increasing J, which is in the downstream direction as required. The condition given by Hayes (1958), that the specific entropy of the material should increase across any gas-dynamic discontinuity if it is to exist, is, perhaps, slightly misleading. Hayes gives several other conditions for the existence of gas-dynamic discontinuities, and in particular he requires that the discontinuity should be externally stable. Only Kahn (1958) has made any attempt to investigate the stability of an ionization front, and he concludes that there are not likely to be any instabilities in practice. Any waviness in the shape of an ionization front will be strongly damped by absorption effects and it is not easy to argue a case for instability if this is taken into account.

Hayes also discusses the possibility of 'internal' instability, and points out that a strong deflagration may be expected to be internally unstable; for any flow pattern containing a strong deflagration is free to drift from one solution to another because it apparently has one degree of indeterminacy. However, this is not the case, for the strong deflagration is internally over-determined (if it can occur at all) and the over-all solution for the flow pattern is unique; thus, internal instability of the type suggested, cannot happen.

The reader is reminded that it has been assumed throughout this paper that shocks can be treated as discontinuities in comparison with the remainder of the wave. This requires that any gradients found in the wave are always very much smaller than gradients found in a shock wave. Thus the arguments used here cannot be applied to a combustion wave if it is only a few mean free paths across. But on the other hand, there is no indication that sufficiently strong relaxation effects will not produce a non-Chapman–Jouguet wave in such a case.

PHILOSOPHICAL TRANSACTIONS OF THE ROYAL SOCIETY A MATHEMATICAL, PHYSICAL & ENGINEERING SCIENCES

It would be interesting to find examples of weak detonations and strong deflagrations to substantiate the theoretical arguments put forward in this paper. However, the problem of devising a combustion process with the required endothermic section may prove rather difficult. The author suggests that some success may possibly be obtained by mixing the combustible gases with a fog of a neutral liquid. This fog would evaporate during the combustion process, giving the necessary cooling effect, and the width of the relaxing region so produced could be varied by altering the density of the fog and the size of the droplets. This mechanism would not work very well if a shock were to propagate ahead of the combustion zone, and a suitable external flow would have to be used to avoid this difficulty. The problem of the external flow is an important one, for it is doubtful if any useful results can be obtained from one-dimensional channels, as the walls produce effects which may change the character of the flow completely. Cylindrical and spherical waves are more likely prospects for this work, as the apparatus should not have such a great effect on the flow pattern as it does in channel flow. Taylor (1950) has given some solutions for the external flow in waves having spherical symmetry,† but this work is not as complete as Goldsworthy's for ionization fronts, and no adequate diagrams are available showing all possible flow pattern solutions, such as figure 1.

In the case of ionization fronts, it is very likely that weak *R*-types and strong *D*-types will be found. Although the flow pattern around any hot star is unsteady, the different types of pattern should be observable in nebulae at various stages of their development. A rough estimate indicates that if the exciting star is of spectral type *O* 6, and it radiates into interstellar gas having a density of about 10 atoms per cubic centimetre, H II regions of diameter up to about 8 parsecs are likely to have a weak *R*-type flow pattern, and those of diameter in the approximate range 8 to 15 parsecs are likely to be strong *D*-type. Larger nebulae are almost certainly weak *D*-type in flow pattern. Weak *R*-type or strong *D*-type flow patterns can be distinguished from weak *D*-type flow patterns by the presence of a shock in the ionized gas, which will cause splitting of the spectral lines emitted by the nebula. This effect has been observed in planetary nebulae, but here the flow pattern is possibly complicated by the ejection of a considerable amount of material from the star itself. This ejection may result in an extra shock facing towards the star, and hence the flow patterns would be rather complex. Planetary nebulae also seem to be strongly affected by magnetic fields in many cases, and it may be difficult to draw any sound conclusions from observations of such nebulae. Satisfactory support for the theoretical work on ionization front propagation must therefore come from observations of relatively small nebulae (less than 15 parsecs in diameter) surrounding the youngest hot stars of population I.

I wish to extend my sincere thanks to Dr F. A. Goldsworthy for his advice and assistance in the preparation of this work. I am indebted to many others for their help at various times, notably Professor M. J. Lighthill, F.R.S., and also Dr F. D. Kahn, Dr W. S. Sargent, Dr J. Hazelhurst, and Dr R. H. Kerr. The work was carried out during a period of scientific training under the sponsorship of the New Zealand Scientific Defence Corps.

† Results similar to Taylor's have been obtained by Zel'dovich, whose work is discussed by Landau & Lifshitz (1959, p. 488).

References

Courant, R. & Friedrichs, K. O. 1948 *Supersonic flow and shock waves*. New York: Interscience.

Crocco, L. 1958 *Fundamentals of gas dynamics*, §B. Princeton University Press.

Goldsworthy, F. A. 1958 *Rev. Mod. Phys.* **30**, 1062.

Goldsworthy, F. A. 1961 *Phil. Trans.* A, **253**, 277 (preceding paper).

Hayes, W. D. 1958 *Fundamentals of gas dynamics*, §D. Princeton University Press.

Kahn, F. D. 1954 *Bull. astr. insts Netherlds*, **12**, 187 (no. 456).

Kahn, F. D. 1955 *Gas dynamics of cosmic clouds* (ed. H. C. Hulst & J. M. Burgers), p. 60. Amsterdam: North-Holland Publishers.

Kahn, F. D. 1958 *Rev. Mod. Phys.* **30**, 1058.

Landau, L. D. & Lifshitz, E. M. 1959 *Fluid mechanics*. London: Pergamon.

Oort, J. & Spitzer, L. 1955 *Astrophys. J.* **121**, 6.

Saunders, O. A. 1953 Chapter 6 of *Modern developments in fluid dynamics* (ed. L. Howarth), vol. 1, 190. Oxford University Press.

Spitzer, L. 1954 *Astrophys. J.* **120**, 5.

Stromgren, B. 1939 *Astrophys. J.* **89**, 526.

Struve, O. & Elvey, C. T. 1938 *Astrophys. J.* **88**, 364.

Taylor, Sir Geoffrey 1950 *Proc. Roy. Soc.* A, **200**, 235.

Taylor, Sir Geoffrey & Tankin, R. S. 1958 *Fundamentals of gas dynamics*, §G. Princeton University Press.

Zel'dovich, Ya. B. 1950 *N.A.C.A. Tech. Mem.* no. 1261.

PHILOSOPHICAL TRANSACTIONS OF THE ROYAL SOCIETY A MATHEMATICAL, PHYSICAL & ENGINEERING SCIENCES